Wiley
Advances in Civil Engineering
Volume 2025, Article ID 4398231, 17 pages
https://doi.org/10.1155/adce/4398231

WILEY

Research Article

Numerical Simulation of Appropriate Design for Selecting Tunnel Support Systems in Squeezing Grounds (Tunnel No. 2 in Tabas Coal Mine, Iran)

Mahdis Shekarchizadeh, Mehdi Najafi, and Mohammad Fatehi Marji

Department of Mining and Metallurgical Engineering, Yazd University, Yazd, Iran

Correspondence should be addressed to Mehdi Najafi; mehdinajafi@yazd.ac.ir

Received 21 June 2024; Accepted 5 March 2025

Academic Editor: Tengfei Nian

Tunnel No. 2 of the mechanized Tabas coal mine and access entry to E5 panel serve as the primary routes for coal extraction from the longwall mining panel. The main objective of this research is to strengthen and select the optimal support system in the area after the intersection of main tunnel No. 2 with the access tunnel E5 panel, using numerical modeling (FLAC 3D software). The results of numerical modeling have indicated that due to coal seam dip and its partial intersection with tunnel No. 2 at the junction of the main tunnel and the eastern access tunnel at levels 2410–2430, along with the presence of the coal seam above this area, there is less rock mass resistance to the induced stresses. Consequently, significant displacements have been occurred in the floor, walls, and roof of the main tunnel. The numerical modeling results indicated displacements of approximately1.4 m in the sidewalls, 0.8 m in the roof, and 1.2 m in the floor, which correlated with the field measurements. The best way to reinforce and optimize the support system was determined by evaluating the supporting effects of mixed support systems, such as truss bolts, flexi bolts, and different steel frames. Therefore, the best support system arrangement was suggested as adding three 6-m-long flexi bolts in the sidewalls and two 3-m-long truss bolts in the tunnel floor, steel frame TH40, eleven 2.7-m rock bolts, and one 9-m cable bolt in the ceiling and walls was proposed. This support system arrangement reduces the tunnel convergence to 90%. This system has been successfully implemented in the mine and reduced the squeezing-related problems to the lowest degree.

Keywords: FLAC3D; numerical modeling; squeezing rock; support system; Tabas coal mine

1. Introduction

Squeezing behavior of rock occurs due to time-dependent convergences and large displacements during tunnel excavation in deep underground mines. This is a condition of instability in tunnels where the rock mass moves inward into the excavated space because of the high induced stresses (produced due to the formation and in situ compressive stresses) which may exceed the rock mass shear strength [1]. The squeezing (time-dependent deformations) of the surrounding rock mass could occur during tunnel excavation and/or over an extended time [2]. The level of tunnel convergence, the rate of displacements, and the extent of the plastic zone around the tunnel depend on the geological and geotechnical properties of the rock mass, in addition to the in-situ stress, water flow, hydrostatic pressure, and rock mass structures [3]. On the other hand, squeezing has a close relationship with excavation methods, the installation time of support systems, and type of support system. For instance, if the support system installation takes longer than the expected time, stresses redistribute and may release, causing the rock mass to move into the tunnel [4]. If the support system is installed hastily without thinking about the required amount of time for stress relief, the system will be under a lot of strain [5]. If design was not correctly implemented, excavation in deformable grounds causes considerable delays in tunnel construction projects and imposes high economic costs. Therefore, improving the support system in mines with

such conditions has a significant positive impact on the safety and financial circumstances of the mine [6]. Determining the most suitable support system is one of the main challenges for engineers because numerous influential factors, such as rock mass parameters, stress conditions, moisture content, and the performance of support systems, significantly impact the selection process [7, 8].

Several numerical methods have been used for investigating the stress concentration and displacement conditions around the tunnels. Finite element method (FEM) [9, 10], finite difference method (FDM) [11–13], and direct and indirect boundary element methods (BEMs) [14–22] have been used in literature for analyzing the stresses and failure zones around underground rock excavations.

Considering the convergence of tunnels, especially those in coal mining, numerous studies have been conducted in the field of improving support systems. Jiao et al. [23] introduced a practical support strategy for the Gobi coal mine roadways. This strategy involved the application of a flexible U-shaped steel frame and filling the area behind the frame with chemical materials, increasing the spacing between the U-shaped support system and adding inverted arc steel at the bottom. This approach aimed to minimize instability issues to the greatest extent possible [23]. Ghadimi, Shahriar, and Jalalifar [24] used numerical approaches and instrumentation tools to create an acceptable pattern for the rock bolt system in the Tabas coal mine. They demonstrated that considering the weak condition of the tunnel's roof, employing 13 mm (in diameter) rock bolts in each row, with a length of 2.4 m, coupled with two cable bolts, each measuring 4 m in length, proved to be the most effective design pattern as compared to other configurations [24]. Akosy et al. [25] used numerical modeling to study the nondeformable support system (NDSS) in tunnel 34 of the Ankara–Istanbul high-speed railway project. Numerical modeling results show that NDSS can give time-dependent solutions. It allows some deformations within the calculated deformation limits rather than zero deformation [25]. Tang et al. [26] proposed a combined support system for excavated roadways in coal mines prone to convergence changes. This support system includes cable bolts, wire mesh, shotcrete, U-shaped steel frames, a layer of foam concrete, and a layer of gravel. The Bbehavior of the support system is explained through numerical analysis and field monitoring. The results have indicated that to use U-shaped steel frames significantly reduces the convergence rate [26]. Wang et al. [27] observed rock collapses surrounding the soft coal mine galleries in their study at Liangjia, China. They noted that rock bolts and arch frames lacked the necessary potential to withstand pressures and primarily led to significant failures. By analyzing the plastic zone area through the high resistance and pressure reduction theory, they introduced the application of a concrete-filled arch frame (CC) support system [27]. Yang et al. [28] found a suitable support solution for the deep tunnel in China's Xin'An coal mine. According to the findings, the rock bolt, cable bolt, wire mesh, and shotcrete + shell combined support system are the best choice for the tunnel [28]. Wang et al. [29] proposed a steel set concrete combination (SSCC) support system for mining tunnels operating under complex geological conditions. Their tests showed that these frames had a better load-bearing capability than the 36U frames [29]. Mansouri Aliabad, Gholamnejad, and Najafi [30] conducted an investigation into the floor convergence in Tabas coal mine using FLAC3D software. The numerical modeling results indicated that the floor convergence value of the tunnel, without considering the support system for the floor and when the advancement effect of the face is not taken into account, is 45 cm. When the face advancement and its effect are considered, the floor convergence gradually increases as the face approaches the observation point. Eventually, the floor convergence reaches 145 cm when the face is within a 5 m distance from the observation point [30]. Ozdogan et al. [31] focused on optimizing the spacing of support systems in the Omler coal mine in Turkey using the method of convergence confinement. The numerical modeling results indicated that the utilization of the GI 120 profile leads to a reduction in displacement levels around the mine roadways [31]. Wang et al. [32] studied the steel frame support system for tunneling in complex conditions, such as tunneling in brittle rocks where the performance of rock anchors is weak, in water-bearing rocks where water causes softening, in great depths and high stress with creep properties, and in challenging mineral conditions. Wang et al. [33] proposed the use of concrete-filled steel tubes (CFSTs) for improving support systems and controlling deformability during construction in the loess tunnel. This method not only reinforces the primary support but also enhances the stress distribution between the primary and secondary support [34]. San et al. [35] proposed a new novel support system titled the Jet Injection Technique for coal tunnels in week rocks. Numerical modeling and field experiments demonstrated that the support system significantly reduces deformation by enhancing load-bearing capacity and redistributing induced stresses [35]. Wu et al. [34] conducted research on the mechanical properties and the influence of tightening and loosening of rock bolts. Based on the results obtained from experiments conducted on samples, they concluded that the quantity of rock bolts and the anchor angle significantly impact the rock bolt installation system [33]. Abassi et al. [36] conducted a series of numerical modeling analyses using FLAC 3D & FLAC 2D software to analyze the stability of main tunnel. The results obtained indicate that the studied tunnels are unstable. The installation of steel frames is highly effective in preventing wall displacement. However, because of concerns with tunnel floor swelling and the existence of conveyor belts and transit rails, effective implementation of these frames is impossible [36]. Rahmanipoor, Faramarzi, and Azhari [37] presented a new method for optimal rock bolt design in the Tabas coal mine's transportation and ventilation tunnels. FLAC3D software was used to do three-dimensional (3D) numerical analysis. According to their findings, employing floor truss fasteners reduces tunnel floor convergence by 40% [37]. Zhang et al. [38] proposed a 3D finite element (FE) model to study the feasibility of strengthening segmental tunnel linings using steel–concrete composites (SCCs). The numerical simulations show that using high-performance

steel shells (HPS) and/or ultra-high-performance concrete (UHPC) is an effective means of enhancing the strengthening effect of SCCs [38]. Liu, Jiang, and Mang [39] found that in engineering practice, tunnel linings should be reinforced before reaching their final state. The timing of strengthening is a critical parameter in the design of the strengthening process. Regarding the utilization efficiency of the steel plate, the results have shown that the earlier the structure is strengthened, the greater the utilization efficiency of the strengthening material [39]. Wang et al. [40] used the SCC method in the design of a large-scale water transfer tunnel support system in China. This study offers valuable insights for the design and construction of water conveyance shield tunnels with triple-layer composite linings, particularly in high-pressure environments [40].

Yao et al. [41] presented the mechanism of instability of the surrounding rock using a combination of numerical simulation methods, model testing, and rock instability criteria. The study demonstrates that the distribution of stress and displacement during tunnel excavation is significantly affected by the presence of laminated joints. Specifically, the thinner the layer thickness, the more pronounced the influence of the laminations, resulting in greater deformation of the surrounding rock [41]. Terron-Almenara et al. [42] found that in the Bergås highway tunnel project in northern Norway, the permanent tunnel support ultimately consisted of ribs of reinforced shotcrete (RRS), fiber-reinforced shotcrete (FRS), and fully grouted steel rebar rock bolts, which replaced the predetermined cast concrete lining traditionally used in soft tunneling conditions.

One of the existing problems in the Tabas mechanized coal mine is squeezing in certain sections of the main tunnel No. 2. Convergence results in significant displacement of tunnel walls and the roof, allowing rock mass to move into the tunnel. This leads to heaving of the tunnel floor and a reduction in the tunnel's cross-sectional area. Additionally, it weakens and damages the support system, alters the shape of steel frames, and causes destruction to the railway installation. The decrease in coal extraction leads to significant expenses for repairing walls and roof, necessitating the reimplementation and optimization of support systems. The main objective of this research is to select the most suitable design for the support system of this section using numerical modeling considering yielding principle. Accordingly, the initial focus is on the numerical analysis of the existing support system in the mine. Following that, strategies such as reducing the spacing of steel frame rows, increasing the length of rock bolts, altering the type of steel frame, using truss bolts in the tunnel floor, and employing a combination of these strategies have been examined. And finally, an appropriate design has been suggested to reinforce the support system to counteract the instability.

2. Tabas Coal Mine

2.1. Geological Coal Mine of Tabas. Based on geological information of Tabas coal mine obtained from boreholes, surface mapping, trenching, and multiple exploratory tunnels, five coal seams have been confirmed in the vertical sections. The total thickness of these seams, from the lower of seam B to the upper of seam D, averages 8 m and primarily consists of alternating layers of coal, argillite, siltstone, and sandstone. The five coal seams from bottom to top are as follows: D, C2, C1, B2, and B1. The most important mineable coal seam in the Parvadeh 1 area is seam C1. This seam is located, on average, 12.9 m below seam C2.

Three inclined main tunnels were excavated to get access to the coal seam in Tabas mechanized coal mine. The main tunnels have been excavated from the outcrop of the C1 seam with a maximum slope of 14°. After that, the region of the extraction panel is ready by diverging from the main gate. Figure 1 shows the positioning of the main tunnel and the access entry to E5 panel, while Figure 2 illustrates the layering around the main tunnel of Tabas coal mine. The average overburden depth from the ground level is 597 m in this section.

The upper coal seam (C2) has a thickness of 0.7 m and the lower coal seam (C1) is 1.9 m in thickness. The main tunnel has been excavated within the siltstone layer to prepare the extraction panel utilizing the longwall mining method. The cross-section area of the main tunnel is horseshoe-shaped with a radius of 2.5 m and a height of 3.5 m, whereas the access entry E5 is triangular in shape. The main tunnel has a downward slope with an angle of 15° concerning the X-axis and 8° concerning the Y-axis.

2.2. Support System in Main Tunnel No. 2. Figure 3 illustrates the support system in the main tunnel, consisting of 10 rock bolts with a diameter of 22 mm and a length of 2.4 m placed in the roof and walls, 9-m-long cable bolts in the roof, 32-mm rock bolts with a length of 1.8 m in the base of the wall arranged at 1-m intervals, TH36 steel frames set 60 cm apart, accompanied by concrete beams and 3.5 cm mesh. The support system at the intersection point of the main tunnel with the E5 access entry (intersection H16), as illustrated in Figure 4, comprises 13 rock bolts of 3 m in length spaced 80 cm apart, 3 flexi bolts of 6 m in the roof, 10 bolts of 2.7 m in the walls, 2 rock bolts of 32 mm in diameter and 1.8 m in length at the base of the walls, and IPB 260 beams placed 80 cm apart to stabilize the roof. Figure 5 shows an overall picture of the support system for the main tunnel and the entry. Three IPB 320 beams have been installed to bolster the system at the access tunnel's entrance.

3. Numerical Modeling With the Explicit FDM Implemented in FLAC3D

The explicit, Lagrangian calculation scheme and the mixed-discretization zoning technique used in FLAC3D ensure that plastic collapse and flow are modeled very accurately. FLAC3D offers an ideal analysis tool for the solution of 3D problems in mining and geotechnical engineering.

3.1. Geometry and Meshing. The initial geometry is block-based and comprises various layers, including siltstone, sandy siltstone, sandstone, and coal seam. The dimensions of this structure are 60 m in length, 75 m in width, and 90 m in height. In this block model, the main tunnel has dimensions of

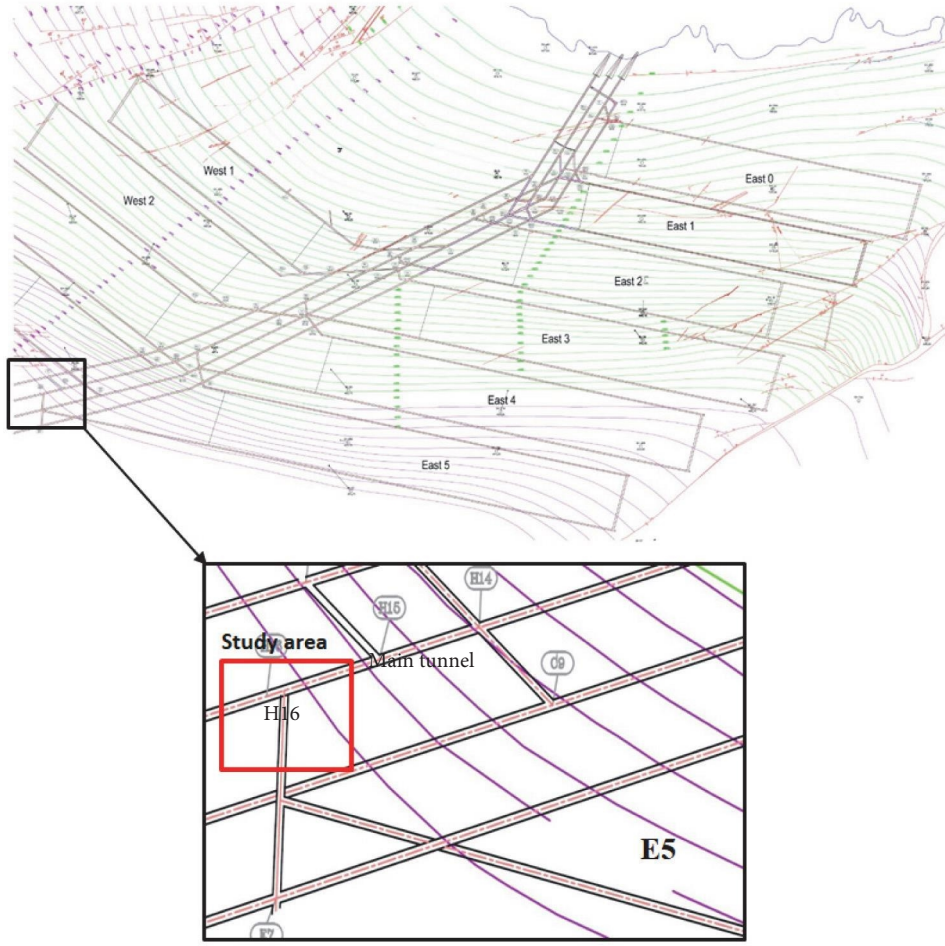

Figure 1: Tunnel No. 2 and access entry E5 (study area) in Tabas mechanized coal mine.

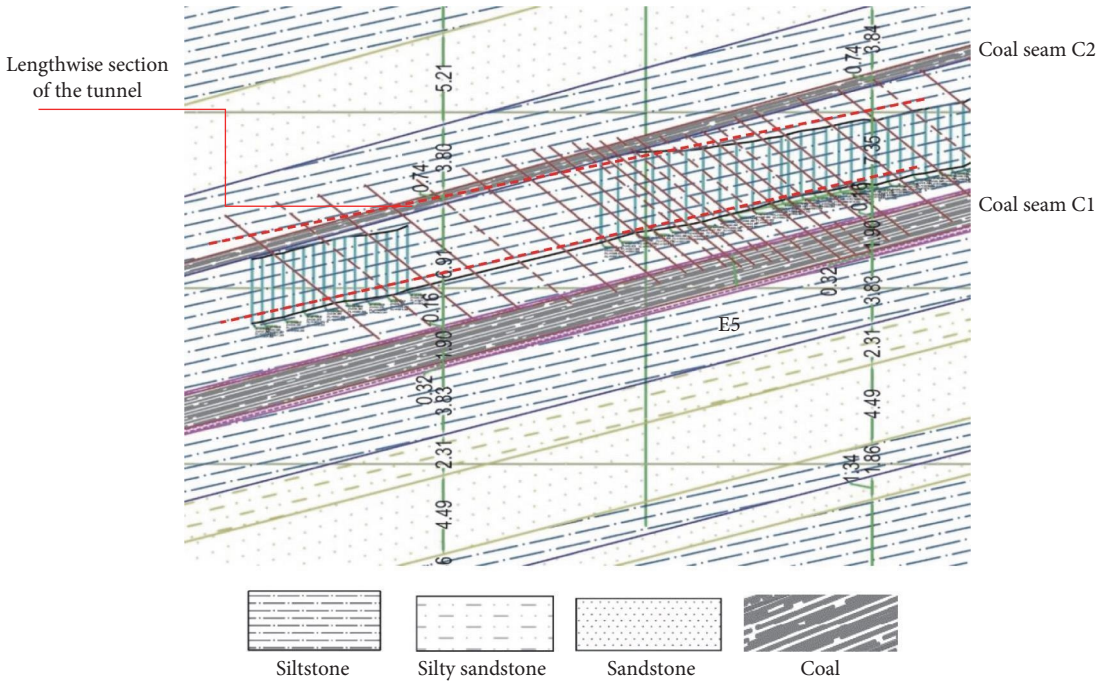

Figure 2: Geological section of tunnel No. 2 in Tabas coal mine (longitudinal section).

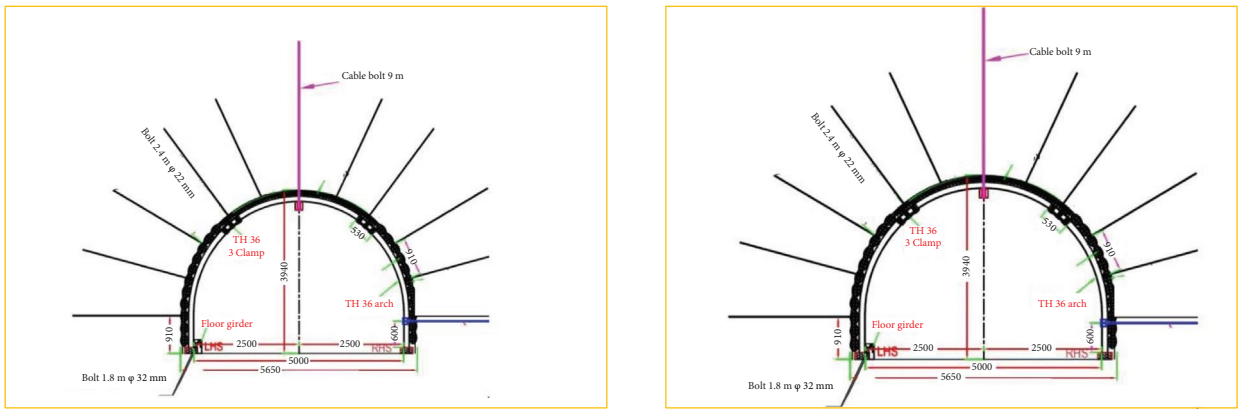

Figure 3: Main tunnel support system.

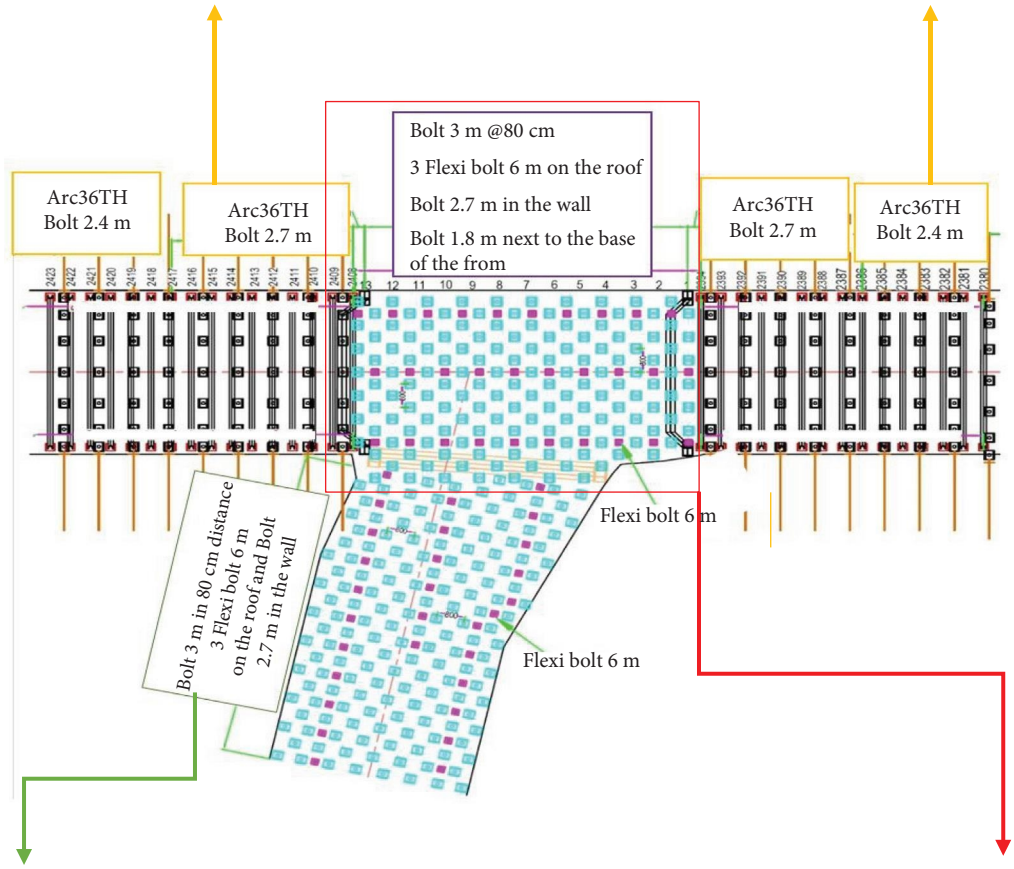

Figure 4: Support system at the intersection of main tunnel No. 2 with access tunnel E5.

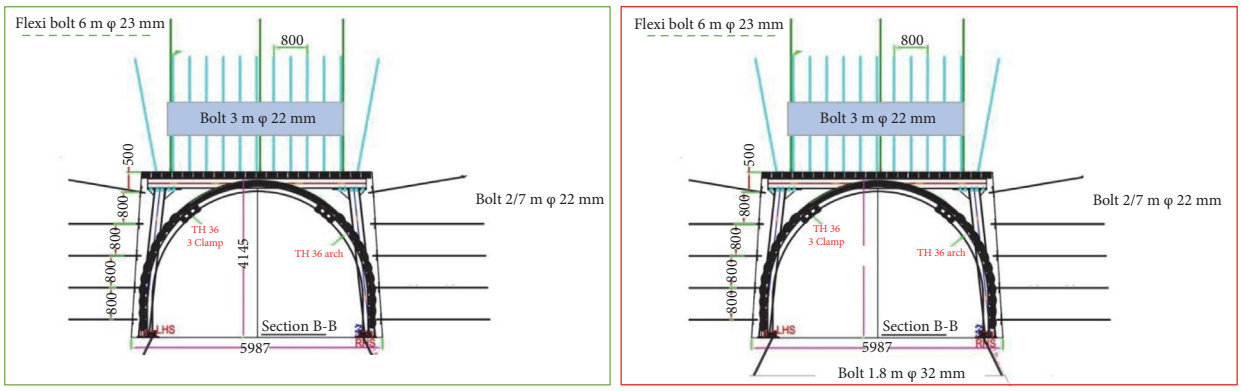

Figure 5: Overview of the support system for the main tunnel No. 2 and access entry E5 panel (plan view).

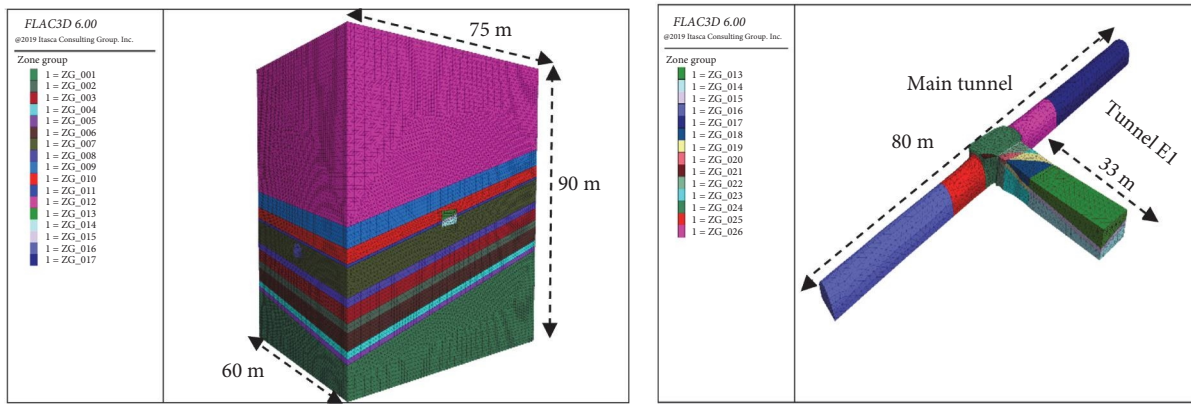

Figure 6: Initial block geometry along with meshing.

Table 1: Characteristics of the rocks surrounding the tunnel [24, 34, 35].

Types of rock	Poisson's ratio	Bulk modulus (GPa)	Shear modulus (GPa)	Cohesion (MPa)	Internal friction angle	Density (kg/m^3)
Siltstone	0.260	1.971	1.126	1.3	24.12	2700
Silty sandstone	0.250	1.991	1.195	0.443	31.75	2500
Coal	0.250	0.211	0.126	0.016	20	1600
Sandstone	0.250	3.521	2.112	8.69	21.75	2700

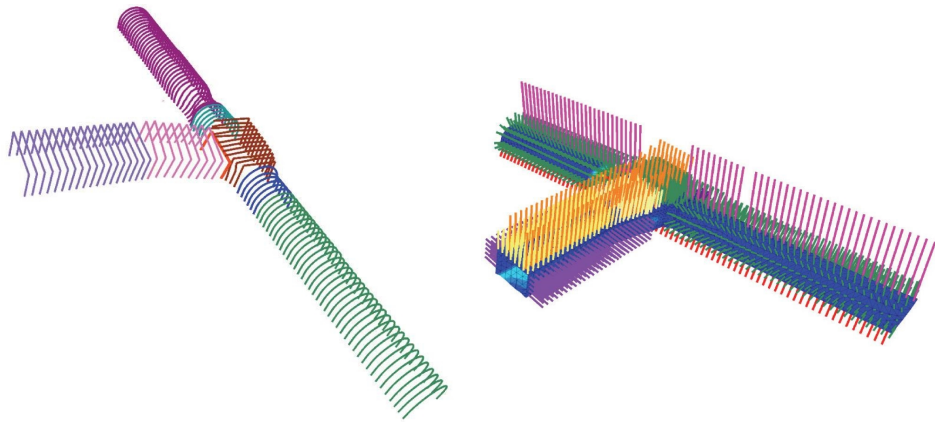

Figure 7: Modeling of the support system for the main tunnel.

80 m in length, an angle of 15° concerning the longitudinal axis, and 8° concerning the transverse axis. Additionally, the access tunnel to the E5 panel, with a length of 30 m, is designed at an angle of 6° from the right wall and 12° from the left wall concerning the longitudinal axis. A three-node mesh has been utilized for the model geometry, effectively covering the environment. The actual overburden at the H16 intersection is 597 m. However, due to computer running time and symmetry condition, in the numerical modeling, 552 m of overburden with an average unite weight of 2.7 ton/m^3 has been considered as an equivalent load, resulting in an applied stress of 14.86 MPa on top of the model. Figure 6 displays both the block model and the tunnel-related model.

3.2. Material Properties. Initially, the Mohr–Coulomb model was used to simulate the behavior of coal seam and roof. Then, for the creep behavior of the coal seam, the Burgers model was utilized. Moreover, the creep properties of coal in Burgers model are E1 = 2.68 GPa, E2 = 12 GPa, $\eta 1 = 0.54$ GPa·h, and $\eta 2 = 24$ GPa·h. These input parameters are shown in Table 1.

3.3. Initial Boundary Conditions. In the initial condition, velocity changes at boundary nodes are prevented using the FIX command, followed by fixing the model along the *X* and *Y* axes and the bottom along the *Z* axis.

3.4. Excavation of Main Tunnel and Support Systems Installation. After achieving equilibrium in the initial model and eliminating displacement and nodal velocities, tunnel excavation and the installation of tunnel support systems have been done. Tunneling advancement is carried out using

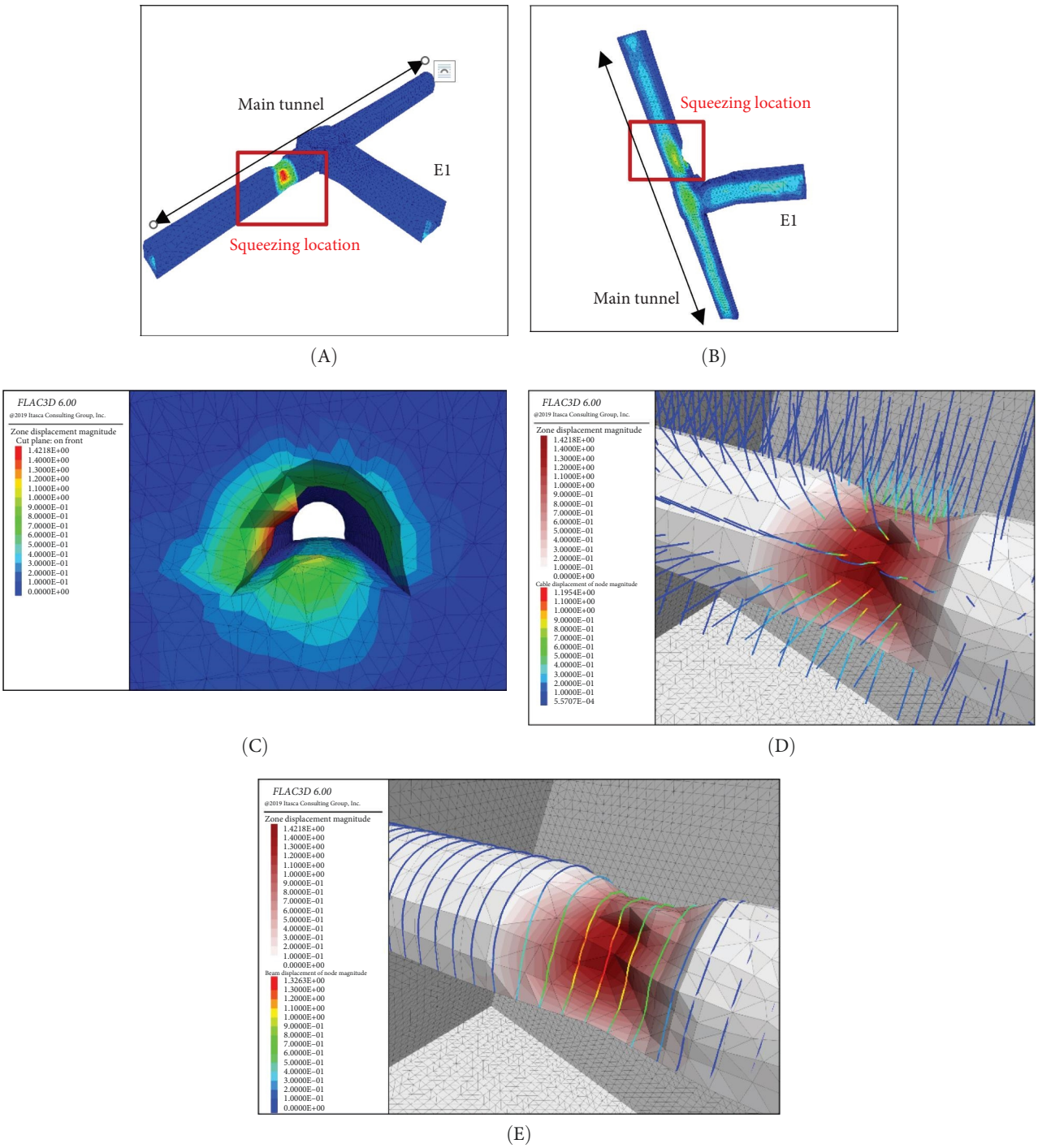

FIGURE 8: Displacements (m) around the main tunnel at the location after the intersection (elevation 2410–2430): (A) around the tunnel, (B) Tunnel floor, (C) Displacements (m) around the main tunnel, (D) displacement of the rock bolts at the location after the intersection (elevation 2410–2430), and (E) displacement of the steel frames at the location after the intersection (elevation 2410–2430).

a roadheader machine in rocky and hard locations, along with drilling and blasting. The control of the advancing face and extraction front, as well as sensitive areas in the mine related to safety, dust, and methane gas emissions, is managed through an advanced monitoring system that utilizes sensors installed at critical points throughout the mine and transmits data to the control room. The extraction areas are located on both sides of these tunnels and are oriented approximately along their length. Main tunnel No. 2 is excavated up to location H16. Then, from the side of tunnel No. 3, access tunnel E5 is excavated toward main tunnel No. 2. Simultaneous drilling has been conducted to connect these two tunnels. The drilling step for the installation of the 60-cm steel frame is specified. The modeling of the support system is illustrated in Figure 7. The displacement around the main tunnel is shown in Figure 8.

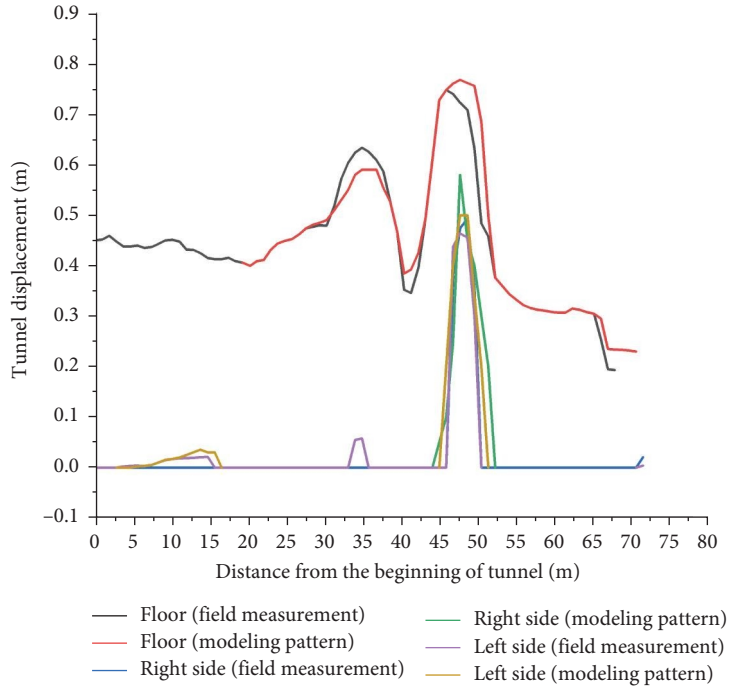

Figure 9: Displacement profile in the tunnel's wall and floor.

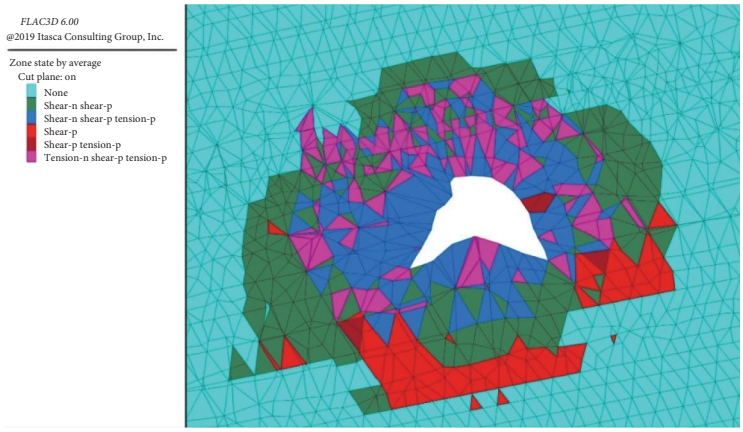

Figure 10: Plastic zone in the area after the H16 intersection.

Figure 9 shows the displacement profile near the floor, roof, and walls along the tunnel length. Based on the available profile, the critical zone of the tunnel appears to be after the H16 intersection, where it's notably evident that the displacement reaches 0.6 m in the walls, 1 m in the roof, and 0.8 m in the floor. Convergence is calculated to be approximately 23% based on a computation of the difference between the initial cross-sectional area of the tunnel (17.6 m^2) and the secondary cross-sectional area of the tunnel (7.96 m^2), divided by the initial cross-sectional area of the tunnel. This convergence is unusually high, implying that the main tunnel faces a danger of closure. The primary reason behind this issue is the passage of the coal seam approximately 1 m above the tunnel and its proximity to the intersection with the east access tunnel. Stress concentration has been notably higher on the left-hand side wall of the tunnel, leading to convergence of the wall and uplifting of the floor as a result.

Figure 10 shows the plastic zone around the tunnel, where the radius of the plastic zone in the area after the intersection is 6 m on the floor, 5 m on the roof, 5 m on the right wall, and 10 m on the left wall. For the coal seam located 1 m above the tunnel, this location is after the intersection of the main tunnel with the access tunnel, so it predicted to the main case of convergence of the walls, roof, and floor occurs. The model created aligns perfectly with the actual condition in the tunnel and Figure 10 illustrates this occurrence.

Results from the numerical model are closely consistent with the convergence recorded in the mine. The displacement values in the mine are 1.35 m for the walls, 80 cm for

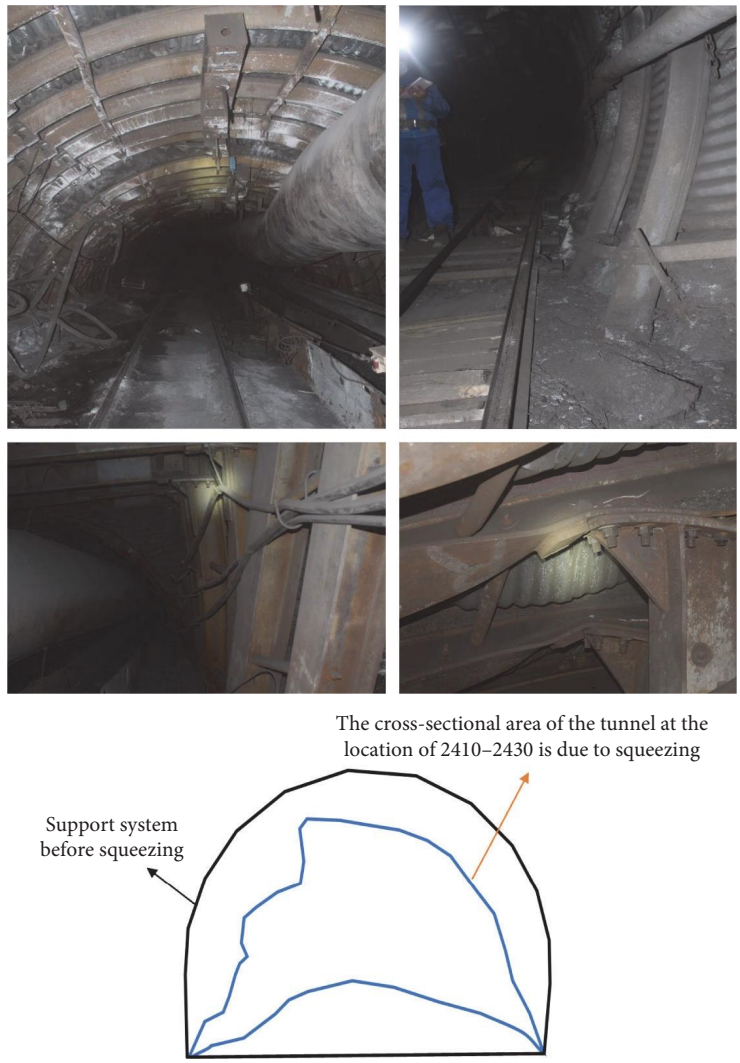

FIGURE 11: Convergence in main tunnel No. 2 of Tabas coal mine.

the roof, and 1.2 m for the floor. The reinforced section at elevations 2410–2430 has a length of 15 m. The squeezing is located in the main tunnel, just after the intersection with the access tunnel. This displacement occurred in the main tunnel No. 2, after the intersection with the access tunnel. Therefore, the tunnel support system, as shown in Figure 3, needs to be modified and reinforced. The convergence of the tunnel in Tabas coal mine is shown in Figure 11. It should be noted that the filed investigation in the mine have shown that the tunnel convergence is more than 45%. The main tunnel and the access tunnel to E5 panel serve as the coal extraction route from the production face using a conveyor belt. They also provide ventilation and pathways for people and other equipment. Issues arising from convergence in the mine result in problems, such as disruptions in traffic, interruptions in the transfer of mineral materials, time-consuming floor cleaning operations, and additional costs due to excessive use of rockbolts. Considering the mentioned issues, the support system at levels 2410–2430 was dismantled, and a new maintenance system was reinstalled.

3.5. The Proposed Support System Strategies for the Stability of the Main Tunnel No.2. Various strategies were investigated consecutively to determine the optimum technique for dealing with the tunnel's high deformability. Ultimately, through the analyses conducted, the best design for reinforcing the support system has been chosen.

3.5.1. Design 1: Using TH40 Steel Frame. In this design, TH40 steel frame was utilized for the frame rather than TH36 in the original support system design (Figure 12A).

3.5.2. Design 2: Reducing the Spacing Between Steel Frame Rows. This design mirrors the initial support system of the mine, with the difference being the utilization of TH36 steel frames spaced 30 cm apart (Figure 12B).

3.5.3. Design 3: Increasing the Length of Rock Bolts. This design is similar to the initial support system of the mine but with the difference that the length of rock bolts used has increased from 2.4 to 2.7 m (Figure 12C).

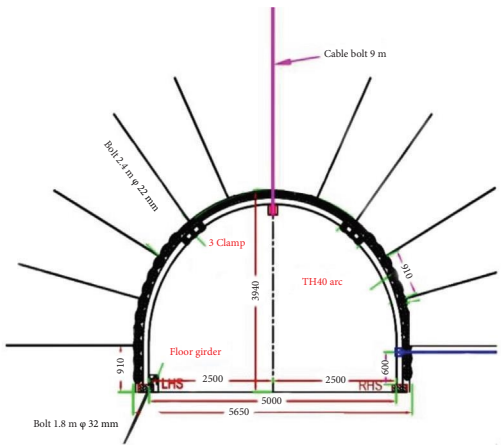

B: Design 1

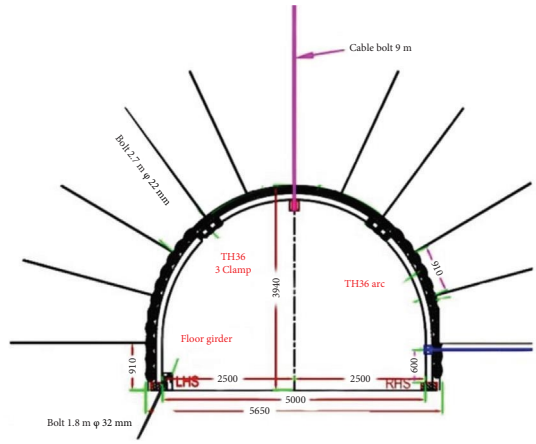

A: Design 2

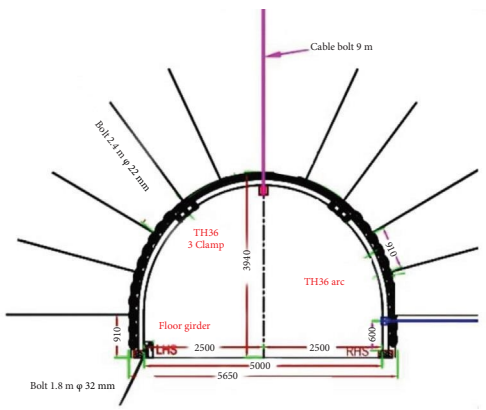

C: Design 3

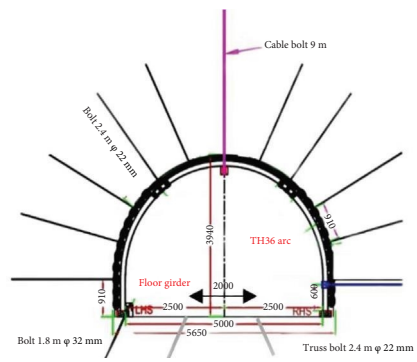

E: Design 4

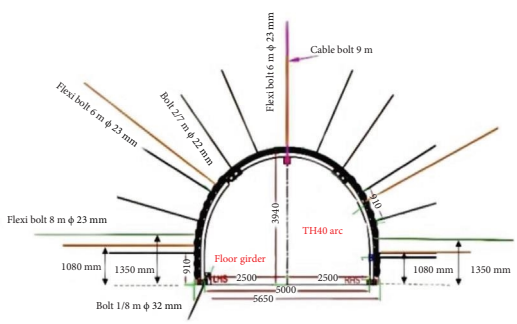

D: Design 5

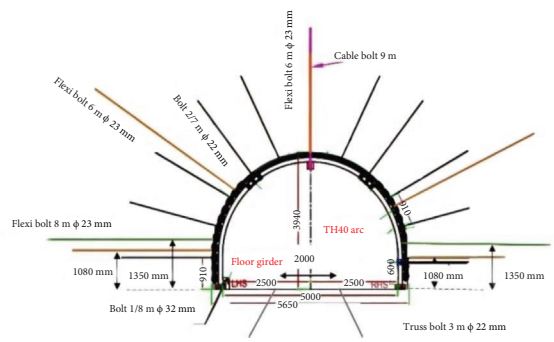

W: Design 6

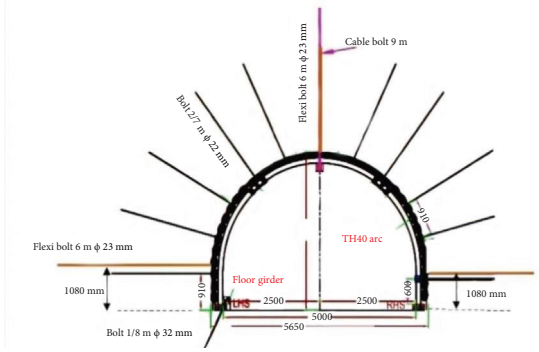

Z: Design 7

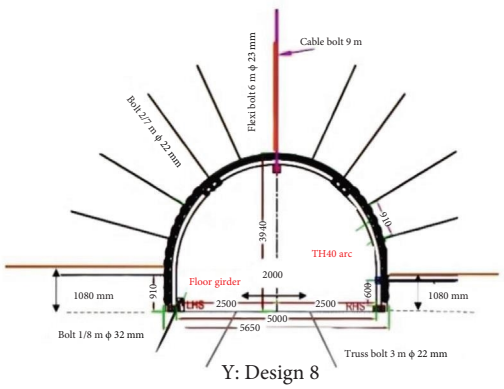

Y: Design 8

FIGURE 12: Layout of the support system in different strategies.

Table 2: Support system design in main tunnel No. 2.

Design no.	Steel frame		Rock bolt		Cable bolt		Truss bolt		Flexi blot	
	Type	Spacing (m)	Length (m)	Spacing (m)	Length (m)	Spacing (m)	Length (m)	Spacing (m)	Length (m)	Spacing (m)
0	TH36	0.6	2.4 1.8	1 1	9	1	—	—	—	—
1	TH40	0.6	2.4 1.8	1 1	9	1	—	—	—	—
2	TH36	0.3	2.4 1.8	1 1	9	1	—	—	—	—
3	TH36	0.6	2.7 1.8	1 1	9	1	—	—	—	—
4	TH36	0.6	2.4 1.8	1 1	9	1	2.4	1	—	—
5	TH40	0.5	2.7 1.8	1 1	9	1	—	—	6 8	1 1
6	TH40	0.5	2.7 1.8	1 1	9	1	3	1	6 8	1 1
7	TH40	0.6	2.7 1.8	1 1	9	1	—	—	6	1
8	TH40	0.6	2.7 1.8	1 1	9	1	3	1	—	1

3.5.4. Design 4: Truss Bolting the Floor at the H16 Intersection. The support system includes the initial pattern along with the floor truss bolt. It utilizes 22 mm diameter rock bolts, 2.4 m in length at a 45° angle, and spaced 2 m apart along the tunnel floor (Figure 12D).

3.5.5. Design 5: Using Flexi Bolts With Length of 6 and 8 m. In this design, 11 rock bolts, each 2.7 m long, along with 9-m-long cable bolts, are used on the roof and walls. Additionally, five flexi bolts, 6 m in length, are installed on the roof and walls. Furthermore, two flexi bolts, 8 m in length, are installed on the left and right walls with a 1-m row spacing. TH40 steel frames are installed spaced 50 cm apart from each other (Figure 12E).

3.5.6. Design 6: Using Flexi Bolts With Lengths of 6 and 8 m and Truss Bolts With the 3 m Length in the Tunnel Floor. This situation is comparable to situation 5, but in this case, 2-floor truss bolts have been installed at a 2-m distance from one another, measuring 3 m in length and angled at a 45° angle with respect to the tunnel floor (Figure 12Y).

3.5.7. Design 7: Using Flexi Bolts With 6 m Length. In this design, 11 rock bolts measuring 2.7 m in length with a diameter of 22 mm are used on the roof and walls. Additionally, a 32-mm rock bolt, 8.1 m in length, is utilized at the base of the left wall. A 9-m-long cable bolt is installed on the roof with a 1-m row spacing. Furthermore, three flexi bolts, 6 m in length, are installed on the walls and roof, along with TH40 steel frames spaced 60 cm apart (Figure 12Y).

3.5.8. Design 8: Using Flexi Bolts With 6 m Length and Truss Bolts With the 3 m Length in the Tunnel Floor. This support system includes 11 rock bolts, 2.7 m in length with a diameter of 22 mm, installed on the roof and walls. A 9-m cable bolt is installed on the roof with a 1-m row spacing from each other. A truss bolt with 3 m length and 22 mm diameter is installed on the floor with a 2 m spacing from each other at a 45° angle relative to the mine floor. Moreover, three flexi bolts, each 6 m length, are positioned on the walls, along with TH40 steel frames spaced 60 cm apart (Figure 12Z).

In Table 2, a summary of proposed support systems is illustrated.

4. Analysis of the Numerical Results

The displacement contours generated in various strategies are illustrated in Figure 13. Based on this figure, the following points are notable:

- The first design: Using the TH40 frame had little impact on the displacement and convergence of the walls, particularly the left wall. It improved the convergence of the tunnel by 5% compared to the initial support system, which was very insignificant.
- The second design: The narrower spacing between the rows of steel frames has reduced displacement around the tunnel. However, significant displacements remain around the tunnel and the amount of convergence has not reached a minimum.
- The third design: Due to the close proximity of the coal seam to the tunnel roof, the increased length of the rock bolts has had an inverse effect on reducing displacement. The primary reason for this issue is the presence of weak layers above the tunnel, situated between the roof and the coal seam layer. This arrangement causes the roof to converge downward. The coal

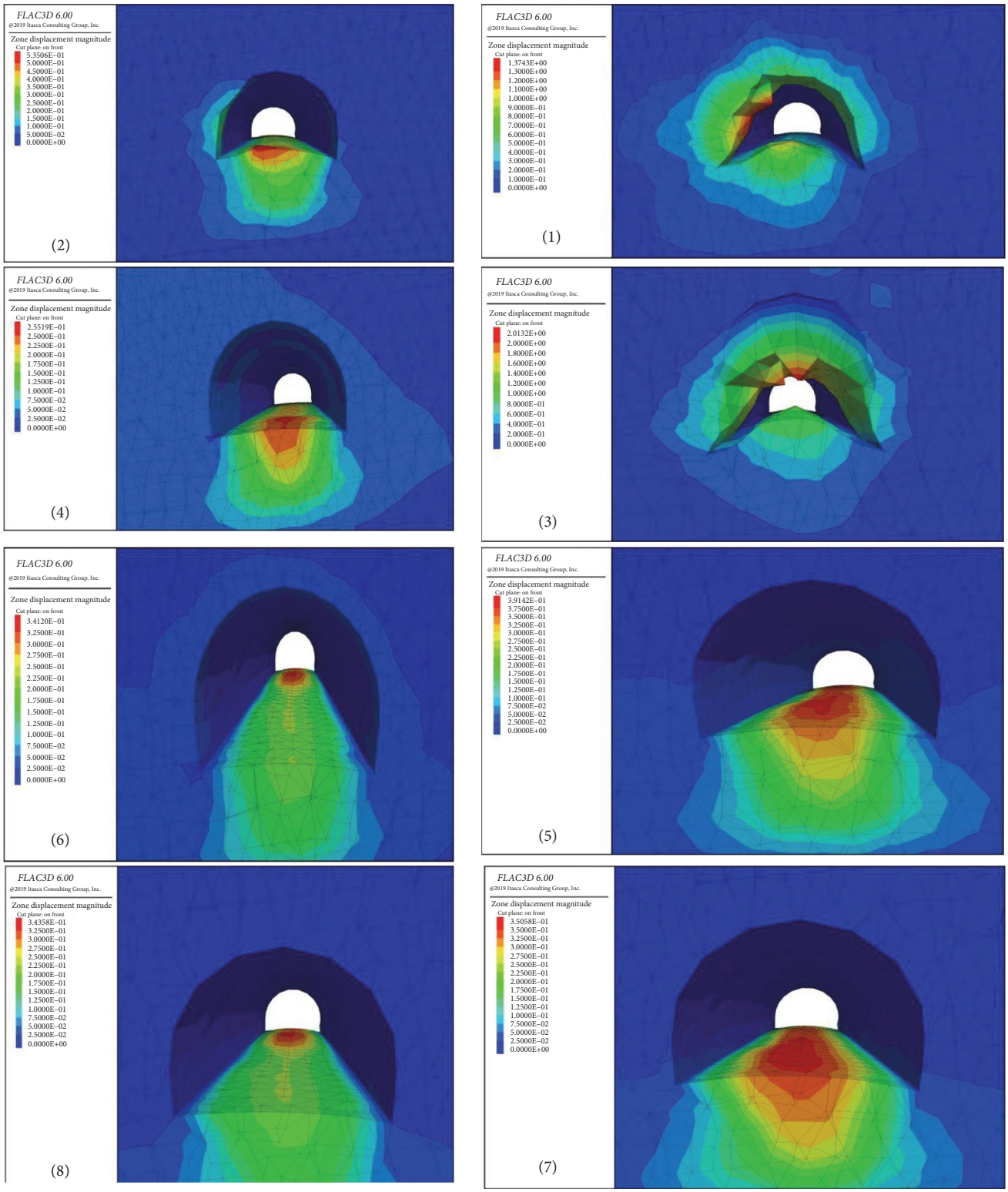

FIGURE 13: Displacement around the main tunnel No.2 in different strategies.

seam layer is also weak and shows creeping behavior, moving toward the tunnel's interior.

- The fourth design: By utilizing truss bolts in the tunnel floor, the displacement near the surrounding tunnel has been significantly reduced, with only an uplift occurring in the floor. However, floor heave in this design has reached its minimum compared to other patterns (0.48 m). This displacement has taken place at the intersection of the access tunnel with the main tunnel, and the reason for this convergence is the lack of reinforcement in the area

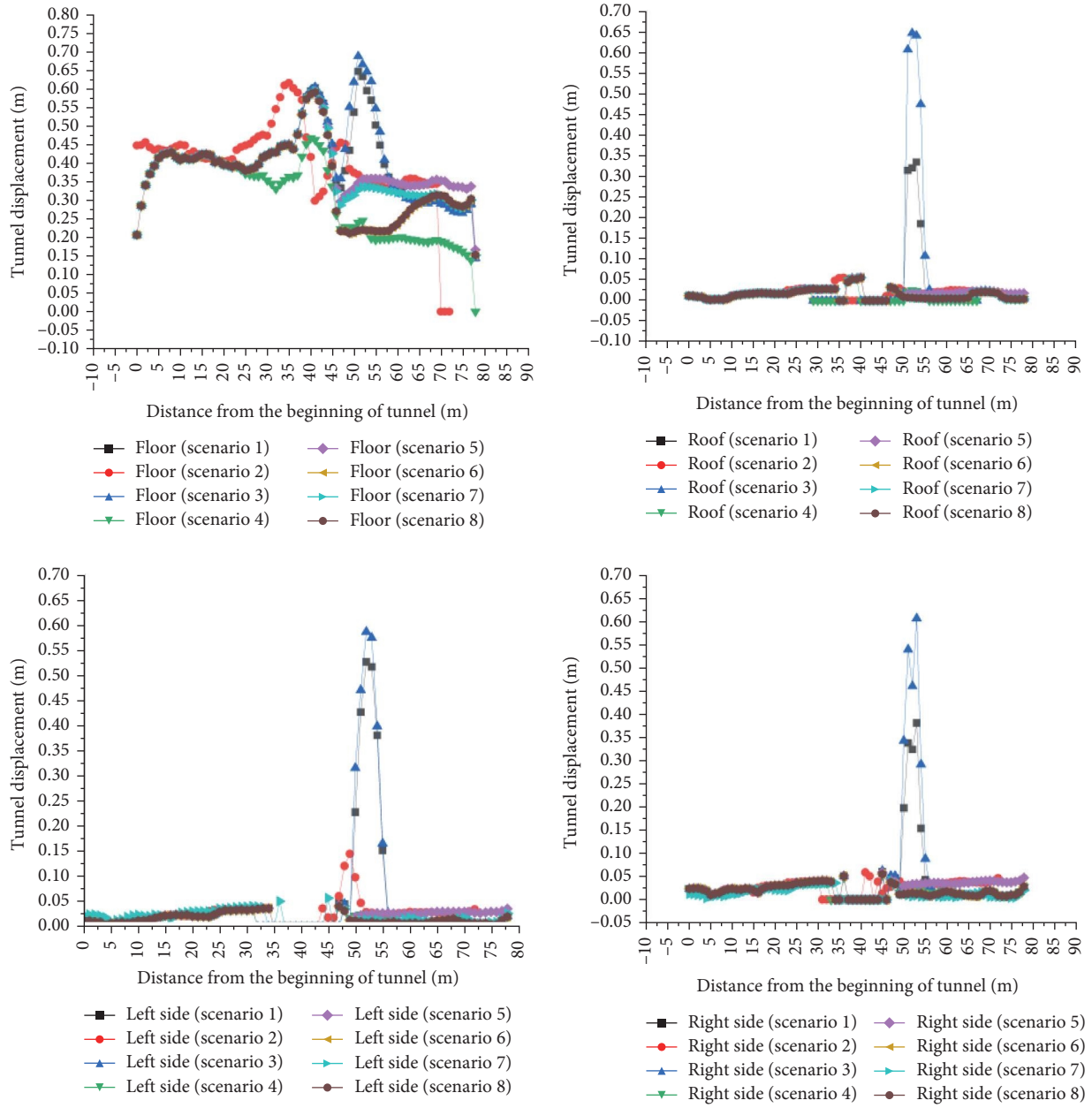

FIGURE 14: Displacement profile along the main tunnel length.

before the intersection. Therefore, this method can be utilized as an efficient approach to prevent tunnel convergence in combination with other methods, aiming to minimize the failure zone as much as possible.

- The fifth design: The use of 6- and 8-m length flexi bolts resulted in the removal of tensile zones in the tunnel's roof, resulting in a considerable reduction in the failure area in both the roof and the walls. However, issues regarding floor heave and uplift persist, and the implementation of this system does not affect the displacement of the tunnel floor.
- The sixth design: The installation of truss bolts in the floor reduces the floor displacement, and no difference in the wall displacement has been observed compared to design 5.
- The seventh design: There has been a significant displacement in the tunnel floor. However, the displacement in the left and right walls, as well as the tunnel's roof, shows minimal changes compared to previous conditions. The primary reason for this is the inclined nature of the tunnel both longitudinally and laterally, along with the proximity of the constrained area to the access tunnel.
- The eighth design: The installation of truss bolts with 6 m length flexi bolts has resulted in reducing the displacements around the tunnel and in the floor.

Table 3: Displacement of main tunnel No. 2 at Elevation 2410–2430 during support system installation.

Design no.	Floor	Roof	Right side wall		Left side wall	
	(m)	(m)	The floor of the tunnel	2 m above the tunnel floor (m)	The floor of the tunnel	2 m above the tunnel floor (m)
0	1.1	0.8	0.3	0.8	0.5	1.4
1	1.1	0.7	0.3	0.8	0.5	1.3
2	0.55	0.10	0.10	0.15	0.15	0.25
3	1.4	2	0.6	1.4	0.8	1.6
4	0.225	0.025	0.05	0.025	0.05	0.025
5	0.35	0.05	0.05	0.05	0.12	0.05
6	0.25	0.05	0.05	0.05	0.05	0.05
7	0.30	0.025	0.10	0.05	0.10	0.05
8	0.20	0.05	0.05	0.025	0.05	0.025

The displacement in the tunnel floor is approximately 20 cm, while in the walls and roof, it is only 2.5 cm. In the critical area, the displacement in the tunnel floor has reached its minimum among other conditions, and the tunnel convergence has decreased by 90% in this state.

To compare the displacement values generated in different strategies, the displacement profile in the roof, right wall, left wall, and tunnel floor has been plotted and is shown in Figure 14. The sudden jump in the graph in the range of 45–60 m from the tunnel entrance is precisely the area where system support needs to be strengthened. This range is between elevations 2410 and 2430, spanning 15 m, located in main tunnel No. 2, after the intersection with the access tunnel. The aim of this research is to investigate the convergence and reinforce the support system in this area. The squeezing has led to a reduction in the tunnel's cross-section, weakening and damaging the support system, deforming steel frames, and damaging the rail system. This has resulted in decreased coal extraction, imposing significant costs for wall and roof repairs, re-execution, and optimization of the tunnel support system. Therefore, it is necessary to predict the convergence rate of the mentioned mine tunnels to develop measures to prevent further convergence in the tunnels.

According to the Figure 14, it is evident that strategies 1 and 3 are not suitable strategies, and practically, in the distance of 45–60 m from the beginning of the tunnel, they did not exhibit satisfactory performance. An important observation is the consistent downward trend in floor heave across different strategies. This trend is more prominent in design 4, where despite the tunnel's inclination in the area following the intersection, the utilization of truss bolts has notably reduced the floor heave.

Considering Figure 14, support system in design 2, hasnot provided adequate reinforcement to prevent convergence in the left wall. However, in design 5, employing flexible bolts for wall stability and preventing convergence has yielded favorable results. The displacement in the tunnel floor in the studied area is approximately 40 cm, whereas in the walls and roof of the tunnel, it is very minimal. The displacement of the right and left tunnel walls at the H16 intersection and level from 2410 to 2430 has reached the minimum possible level, and convergence has been well controlled. Therefore, the use of flexi bolts is highly effective. However, there was still some floor heave present. Hence, in design 6, trussbolts and flexi bolts were used, resulting in favorable outcomes.

The mining support system needs to be both financially feasible and sustainable. Therefore, design 7 has been proposed. By reducing the number of flexi bolts used in the walls and roof, as depicted in Figure 14, tunnel convergence can be controlled within this range. However, the reduction in floor uplift remains unchanged.

By examining various strategies, we have understood that using 6- and 8-m-long flexi bolts leads to the removal of shear zones in the tunnel roof and significantly reduces the fractured area in the roof and walls. In design 8, the installation of 6-m flexi bolts and truss bolts has resulted in the minimum level of convergence and uplift in the floor.

The displacement measurements at various tunnel positions are shown in Table 3 to estimate displacement values across strategies. Design 8 was selected as the best-performing design since it is clear from the table that it is superior to the other designs.

5. Conclusion

In this study, considering the significant convergence issues in main tunnel No. 2 of the Tabas coal mine, support system analysis was conducted using FLAC3D software at the intersection of the main tunnel with the access tunnel of panel E5. The behavioral model used was initially analyzed under Mohr–Coulomb conditions to observe the unbalanced forces. Then, in the plastic state and considering the creep of the coal seam, the Mohr–Coulomb model was used for all layers of siltstone, silty sandstone, and sandstone, while the Burgers model was applied for coal.

Initially, the support system used in the Tabas coal mine was modeled. The results showed that the highest level of convergence occurred in the area after the intersection of the main corridor with the access tunnel of the eastern section. The uplift of main tunnel No. 2 after the intersection (elevation 2410–2430) measured 1.1 m at the floor, 1.4 m at the left

wall, and 80 cm at the roof. The installed support system is not effective due to the strength and position of the tunnel, as it has experienced severe collapses, making the path for the conveyor belt, ventilation, and traffic very unsuitable. Consequently, by calculating the difference between the initial cross-section area of the tunnel (17.6 m^2) and the secondary cross-section area of the tunnel (7.96 m^2) and dividing it by the initial cross-section area, the convergence was calculated to be 45.23%, which is a very high value and poses a risk of closing the main tunnel. Therefore, it is necessary to implement measures to prevent further convergence of the tunnels. It is worth mentioning that the results of the numerical model are consistent with field observations and the results of monitoring instruments.

The combined support system strategies were considered, incorporating the use of TH40 steel frames, reducing the spacing between steel frame rows, and increasing rock bolt length, truss bolts in the floor, and so forth. Based on these strategies, the research findings are as follows:

1. Using TH40 steel frames instead of TH36, increasing the length of rock bolts, and decreasing rock bolt row spacing did not result in substantial changes in tunnel convergence.
2. Strengthening the tunnel floor with truss bolts has been highly effective in reducing the convergence of the roof and walls, along with decreasing floor uplift and wall displacements. However, the achieved reduction is not satisfactory, indicating the necessity for further reinforcement of the support system.
3. Increase in bolt length: The amount of displacement and the range of the plastic zone have increased because the coal seam is located very close to the top of the tunnel. This increase in bolt length has caused the upper layers of the tunnel, which are situated between the roof and the coal seam, to become weaker and move downward. Additionally, the coal seam, which is very weak and has a creeping behavior, moves toward the inside of the tunnel. For this reason, it leads to the weakening and an increase in the failure zone extending up to the upper region of the coal seam.
4. With the increase in bolt length and the reduction of the spacing between steel frames, the displacement of the roof and walls reaches its minimum value. Therefore, at this stage, the most effective step for reducing the convergence of the roof and walls is to increase the load-bearing capacity of the roof, and the best method for floor heave is the use of truss bolts. The use of truss bolts has somewhat reduced the failure zone in the floor, but it still does not fully impact the convergence of the roof and walls. For this reason, the use of flexible bolts in the walls is recommended.
5. Utilization of flexi bolts with 6 and 8 m lengths resulted in reducing approximately 80% of the convergence in the tunnel walls and roof. This could potentially be considered an effective solution worth exploring. Therefore, installation of flexi bolts with 6 and 8 m lengths was considered the optimal choice for assessing the suitable length and optimal quantity within the framework of comparing the fifth and seventh design strategies of support systems.
6. In the eighth design, the utilization of three 6-m length flexi bolts on the tunnel wall and roof, along with two 3-m truss bolts positioned at a 45° angle relative to the floor, accompanied by TH40 steel frames, cable bolts, and rock bolts in the wall and roof, resulted in a significantly more limited fractured area compared to other support systems. Additionally, from an economic standpoint, fewer flexi bolts were used in this pattern compared to others.
7. In the eighth design of support system, the plastic zone radius in the tunnel floor decreased from 6 to 4 m, and in the roof and walls, the plastic zone reached zero. The results indicate that within the range of 45–60 m from the tunnel entrance, tunnel convergence has decreased by 90%. The cross-sectional convergence in this design stands at 6%. Therefore, this pattern can be considered the most suitable support system. The support system pattern presented in this study was implemented by the Tabas mine management and the technical office and compared with the numerical results. Therefore, it is worth noting that the results of the numerical model are consistent with field observations and the results of the instrumentation.

Data Availability Statement

The data are available upon request to the corresponding author.

Ethics Statement

The authors state that the research was conducted according to ethical standards.

Conflicts of Interest

The authors declare no conflicts of interest.

Funding

No funding was received for this research.

References

[1] S. Jin and W. Lianguo, "Numerical Simulation of Grooving Method for Floor Heave Control in Soft Rock Roadway," *Mining Science and Technology (China)* 21, no. 1 (2011): 49–56.

[2] Y. Sun, J. Zhang, G. Li, et al., "Determination of Young's Modulus of Jet Grouted Coalcretes Using an Intelligent Model," *Engineering Geology* 252 (2019): 43–53.

[3] J. Kang, F. Zhou, C. Liu, and Y. Liu, "A Fractional Non-Linear Creep Model for Coal Considering Damage Effect and Experimental Validation," *International Journal of Non-Linear Mechanics* 76 (2015): 20–28.

[4] E. Karampinos, J. Hadjigeorgiou, and P. Turcotte, "Discrete Element Modelling of the Influence of Reinforcement in Structurally Controlled Squeezing Mechanisms in a Hard Rock Mine," *Rock Mechanics and Rock Engineering* 49, no. 12 (2016): 4869–4892.

[5] M. H. Salimian, A. Baghbanan, H. Hashemolhosseini, M. Dehghanipoodeh, and S. Norouzi, "Effect of Grouting on Shear Behavior of Rock Joint," *International Journal of Rock Mechanics and Mining Sciences* 98 (2017): 159–166.

[6] M. Zare, M. Najafi, J. Gholamnejad, and A. Rooh, "Determination of Suitable Barrier Pillar Width in Tabas Mechanized Coal Mine Using Numerical Modeling," *Tunneling and Underground Space Engineering* 8, no. 2 (2019): 183–201.

[7] W. Li, N. Yang, B. Yang, et al., "An Improved Numerical Simulation Approach for Arch-Bolt Supported Tunnels With Large Deformation," *Tunnelling and Underground Space Technology* 77 (2018): 1–12.

[8] P. Lin, H. Liu, and W. Zhou, "Experimental Study on Failure Behaviour of Deep Tunnels Under High in-Situ Stresses," *Tunnelling and Underground Space Technology* 46 (2015): 28–45.

[9] T. P. Fries and T. Belytschko, "The Generalized/Extended Finite Element Method: An Overview of the Method and Its Applications," *International Journal for Numerical Methods in Engineering* 84, no. 3 (2010): 253–304.

[10] T. Saksala, "Rate-Dependent Embedded Discontinuity Approach Incorporating Heterogeneity for Numerical Modeling of Rock Fracture," *Rock Mechanics and Rock Engineering* 48, no. 4 (2015): 1605–1622.

[11] M. S. Abdollahi, M. Najafi, A. Y. Bafghi, and M. F. Marji, "A 3D Numerical Model to Determine Suitable Reinforcement Strategies for Passing TBM Through a Fault Zone, a Case Study: Safaroud Water Transmission Tunnel, Iran," *Tunnelling and Underground Space Technology* 88 (2019): 186–199.

[12] T. Saksala, D. Brancherie, I. Harari, and A. Ibrahimbegovic, "Combined Continuum Damage-Embedded Discontinuity Model for Explicit Dynamic Fracture Analyses of Quasi-Brittle Materials," *International Journal for Numerical Methods in Engineering* 101, no. 3 (2015): 230–250.

[13] P. A. Cundall, "Formulation of a Three-Dimensional Distinct Element Model—Part I. A Scheme to Detect and Represent Contacts in a System Composed of Many Polyhedral Blocks," *International Journal of Rock Mechanics and Mining Sciences & Geomechanics Abstracts* 25, no. 3 (1988): 107–116.

[14] O. K. Mahabadi, A. Lisjak, A. Munjiza, and G. Grasselli, "Y-Geo: New Combined Finite-Discrete Element Numerical Code for Geomechanical Applications," *International Journal of Geomechanics* 12, no. 6 (2012): 676–688.

[15] A. Lisjak, Q. Liu, Q. Zhao, O. K. Mahabadi, and G. Grasselli, "Numerical Simulation of Acoustic Emission in Brittle Rocks by Two-Dimensional Finite-Discrete Element Analysis," *Geophysical Journal International* 195, no. 1 (2013): 423–443.

[16] H. Smoljanović, N. Živaljić, and Ž. Nikolić, "A Combined Finite-Discrete Element Analysis of Dry Stone Masonry Structures," *Engineering Structures* 52 (2013): 89–100.

[17] N. Zivaljic, H. Smoljanovic, and Z. Nikolic, "A Combined Finite-Discrete Element Model for RC Structures Under Dynamic Loading," *Engineering Computations* 30, no. 7 (2013): 982–1010.

[18] S. L. Crouch and A. M. Starfield, *Boundary Element Methods in Solid Mechanics* (George Allen & Unwin, London, 1983).

[19] M. Cerrolaza and R. Garcia, "Boundary Elements and Damage Mechanics to Analyze Excavations in Rock Mass," *Engineering Analysis with Boundary Elements* 20, no. 1 (1997): 1–16.

[20] N. Nikadat, M. Fatehi, and A. Abdollahipour, "Numerical Modelling of Stress Analysis Around Rectangular Tunnels With Large Discontinuities (fault) by a Hybridized Indirect BEM," *Journal of Central South University* 22, no. 11 (2015): 4291–4299.

[21] N. Nikadat and M. F. Marji, "Analysis of Stress Distribution Around Tunnels by Hybridized FSM and DDM Considering the Influences of Joints Parameters," *Geomechanics and Engineering* 11, no. 2 (2016): 269–288.

[22] A. Abdollahipour and M. Fatehi Marji, "A Thermo-Hydromechanical Displacement Discontinuity Method to Model Fractures in High-Pressure, High-Temperature Environments," *Renewable Energy* 153 (2020): 1488–1503.

[23] Y.-Y. Jiao, L. Song, X.-Z. Wang, and A. Coffi Adoko, "Improvement of the U-Shaped Steel Sets for Supporting the Roadways in Loose Thick Coal Seam," *International Journal of Rock Mechanics and Mining Sciences* 60 (2013): 19–25.

[24] M. Ghadimi, K. Shahriar, and H. Jalalifar, "Study of Fully Grouted Rock Bolt in Tabas Coal Mine Using Numerical and Instrumentation Methods," *Arabian Journal for Science and Engineering* 41, no. 6 (2016): 2305–2313.

[25] C. O. Aksoy, G. G. Uyar, E. Posluk, K. Ogul, I. Topal, and K. Kucuk, "Non-Deformable Support System Application at Tunnel-34 of Ankara-Istanbul High Speed Railway Project," *Structural Engineering and Mechanics* 58, no. 5 (2016): 869–886.

[26] X. Tan, W. Chen, H. Liu, et al., "A Combined Supporting System Based on Foamed Concrete and U-Shaped Steel for Underground Coal Mine Roadways Undergoing Large Deformations," *Tunnelling and Underground Space Technology* 68 (2017): 196–210.

[27] Q. Wang, R. Pan, B. Jiang, et al., "Study on Failure Mechanism of Roadway With Soft Rock in Deep Coal Mine and Confined Concrete Support System," *Engineering Failure Analysis* 81 (2017): 155–177.

[28] S.-Q. Yang, M. Chen, H.-W. Jing, K.-F. Chen, and B. Meng, "A Case Study on Large Deformation Failure Mechanism of Deep Soft Rock Roadway in Xin'An Coal Mine, China," *Engineering Geology* 217 (2017): 89–101.

[29] Q. Wang, B. Jiang, Y. Li, et al., "Mechanical Behaviors Analysis on a Square-Steel-Confined-Concrete Arch Centering and Its Engineering Application in a Mining Project," *European Journal of Environmental and Civil Engineering* 21, no. 4 (2017): 389–411.

[30] H. Mansouri Aliabad, J. Gholamnejad, and M. Najafi, "Numerical Modeling of Tunnel Floor Heave in Tabas Mechanized Coal Mine," *Tunneling and Underground Space Engineering* 5, no. 2 (2016): 15–29.

[31] M. V. Ozdogan, H. Yenice, A. Gönen, and D. Karakus, "Optimal Support Spacing for Steel Sets: Omerler Underground Coal Mine in Western Turkey," *International Journal of Geomechanics* 18, no. 2 (2018): 05017003.

[32] X. Wang, J. Lai, R. S. Garnes, and Y. Luo, "Support System for Tunnelling in Squeezing Ground of Qingling-Daba Mountainous Area: A Case Study From Soft Rock Tunnels," *Advances in Civil Engineering* 2019 (2019): 8682535, 17.

[33] Z. Wang, Y. Xie, H. Liu, and Z. Feng, "Analysis on Deformation and Structural Safety of a Novel Concrete-Filled Steel Tube Support System in Loess Tunnel," *European Journal of Environmental and Civil Engineering* 25, no. 1 (2021): 39–59.

[34] G. Wu, W. Yu, J. Zuo, and S. Du, "Experimental and Theoretical Investigation on Mechanisms Performance of the Rock-Coal-Bolt (RCB) Composite System," *International Journal of Mining Science and Technology* 30, no. 6 (2020): 759–768.

[35] Y. Sun, G. Li, J. Zhang, and D. Qian, "Experimental and Numerical Investigation on a Novel Support System for Controlling Roadway Deformation in Underground Coal Mines," *Energy Science & Engineering* 8, no. 2 (2020): 490–500.
[36] F. Abbasi, M. H. Khosravi, A. Jafari, A. Bashari, and B. Alipenhani, "Support Analysis of Main Tunnels in Tabas Mechanized Parvadeh Mine at Intersection With Coal Seam," *Journal of Mining and Environment* 12, no. 3 (2021): 711–724.
[37] M. Rahmanipoor, L. Faramarzi, and A. Azhari, "A New Rock-Bolting Pattern Proposed for Tabas Fully Mechanized Mine Using Field Instrumentation and Numerical Modelling," *Geotechnical and Geological Engineering* 40, no. 2 (2022): 945–975.
[38] J.-L. Zhang, X. Liu, T.-Y. Ren, Y.-M. Shi, and Y. Yuan, "Numerical Analysis of Tunnel Segments Strengthened by Steel–Concrete Composites," *Underground Space* 7, no. 6 (2022): 1115–1124.
[39] X. Liu, Z. Jiang, and H. A. Mang, "Experimental Investigation of the Influence of the Timing of Strengthening on the Structural Behavior of Segmental Tunnel Linings," *Engineering Structures* 274 (2023): 115070.
[40] D. Y. Wang, H. H. Zhu, X. H. Zhang, et al., "Structural Behavior of Triple-Layer Composite Lining of a Water Conveyance Tunnel: Insight From Full-Scale Loading Tests," *Journal of Rock Mechanics and Geotechnical Engineering* (2024): 1674–7755.
[41] J. Yao, N. Jiang, Y. Yao, C. Zhou, and Y. Yang, "Instability Mechanism of Layered Surrounding Rock Tunnels Affected by Layer Thickness Under Dynamic and Static Loads," *Alexandria Engineering Journal* 105 (2024): 471–484.
[42] J. Terron-Almenara, K. G. Holter, P. D. Jakobsen, B. Aagaard, and A. K. Lund, "Permanent Tunnel Support With Reinforced Shotcrete Arches and Forepoling in Over-Consolidated Till and Weathered Rock. A Case Study Based on the Construction of the Bergås Tunnel, Norway, Tunn," *Tunnelling and Underground Space Technology* 157 (2025): 106256.